

Electronic Supplementary Information

for

Dissipative Control of the Fluorescence of a 1,3-Dipyrenyl Calix[4]arene in the Cone Conformation

Emanuele Spatola,^{a,†} Francesco Rispoli,^{b,†} Daniele Del Giudice,^{a,†} Roberta Cacciapaglia,^a Alessandro Casnati,^b Luciano Marchiò,^b Laura Baldini^{*,b} and Stefano Di Stefano^{*,a}

Index

1. X-ray Diffraction	S1
2. Spectra	S4
2.1 NMR Spectra	
2.1.1. ^1H NMR spectrum of 7	
2.1.2. ^{13}C NMR spectrum of 7	
2.1.3. ^1H NMR spectrum of 3	
2.1.4. ^{13}C NMR spectrum of 3	
2.1.5. ^1H NMR Monitoring of the Reaction between 2.0 mM 3 and 4.0 mM 2	
2.1.6. ^1H NMR Monitoring of the Reaction between 2.0 mM 3 and 10.0 mM 2	
2.1.7. ^1H NMR Monitoring of the Reaction between 2.0 mM 3 and 4.6 mM 4	
2.1.8. ^1H NMR Monitoring of the Reaction between 2.0 mM 3 and 8.0 mM 4	
2.1.9. Comparison between ^1H NMR of 3 after addition of CF_3COH and $\text{CCl}_3\text{CO}_2\text{H}$	
2.2 Emission Spectra	
2.2.1. Fluorescence emission spectrum of 0.15 mM 3 (slit 1 nm)	
2.2.2. Fluorescence emission spectrum of 0.15 mM 7 (slit 1 nm)	
2.2.3. Fluorescence emission spectrum of 5.0 μM 3 (slit 1 nm)	
2.2.4. Fluorescence emission spectrum of 5.0 μM 7 (slit 1 nm)	
2.2.5. Fluorescence emission spectrum of 5.0 μM 7 (slit 5 nm)	
2.2.6. Fluorescence emission spectrum of 2.50 μM 3 + 2.50 μM $\text{CF}_3\text{CO}_2\text{H}$ (slit 1 nm)	
2.3 UV-Vis absorption spectra	
2.3.1 UV-Vis absorption spectra of 2.50 μM 3 in the presence and absence of 2.50 μM $\text{CF}_3\text{CO}_2\text{H}$	
2.4 Excitation Spectra	
2.4.1 UV-Vis excitation spectra of 2.50 μM 3 + 2.50 μM $\text{CF}_3\text{CO}_2\text{H}$	
3. References	S18

1. X-ray Diffraction

A summary of data collection and structure refinement for calixarene **7** is reported in Table 1. Single crystal data were collected with a *Bruker D8 PhotonII*, Mo K α : $\lambda = 0.71073 \text{ \AA}$. The intensity data were integrated from several series of exposure frames covering the sphere of reciprocal space,² and the absorption correction was applied using the program SADABS.³ The structures were solved with the ShelXT⁴ structure solution program and refined with the ShelXL⁴ refinement package using Least Squares minimisation. Graphical material was prepared with the Mercury 4.0 program.⁵ CCDC 2108932 contains the supplementary crystallographic data for this paper. The data can be obtained free of charge from The Cambridge Crystallographic Data Centre via www.ccdc.cam.ac.uk/structures.

Table 1. Crystal data and structure refinement for calixarene 7

Empirical formula	C ₇₆ H ₇₀ N ₂ O ₁₂
Formula weight	1203.34
Temperature/K	150.0
Crystal system	triclinic
Space group	P-1
a/Å	14.238(3)
b/Å	14.993(3)
c/Å	15.638(2)
α/°	70.194(7)
β/°	85.592(7)
γ/°	77.672(8)
Volume/Å ³	3068.1(9)
Z	2
ρ _{calc} g/cm ³	1.303
μ/mm ⁻¹	0.709
F(000)	1272.0
Crystal size/mm ³	0.11 × 0.03 × 0.03
Radiation	CuKα ($\lambda = 1.54178 \text{ \AA}$)
2Θ range for data collection/°	7.18 to 136.48
Index ranges	-17 ≤ h ≤ 16, -18 ≤ k ≤ 18, -18 ≤ l ≤ 18
Reflections collected	37030
Independent reflections	11007 [R _{int} = 0.1530, R _{sigma} = 0.1346]
Data/restraints/parameters	11007/37/843
Goodness-of-fit on F ²	1.017
Final R indexes [I>=2σ (I)]	R ₁ = 0.0790, wR ₂ = 0.1737
Final R indexes [all data]	R ₁ = 0.1757, wR ₂ = 0.2211
Largest diff. peak/hole / e Å ⁻³	0.28/-0.34

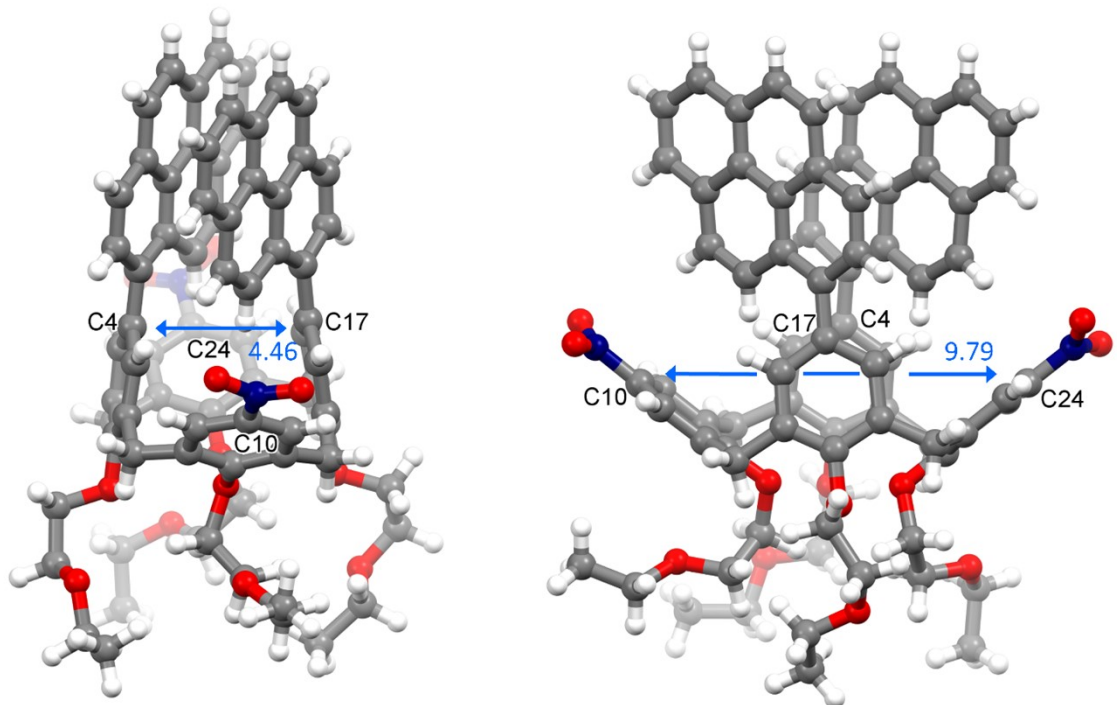


Fig. S1. Molecular structure of **7**, displaying a pinched-cone conformation. The intramolecular distance between C(4) and C(17) is of 4.46 Å, whereas C(10) and C(24) are separated by 9.79 Å.

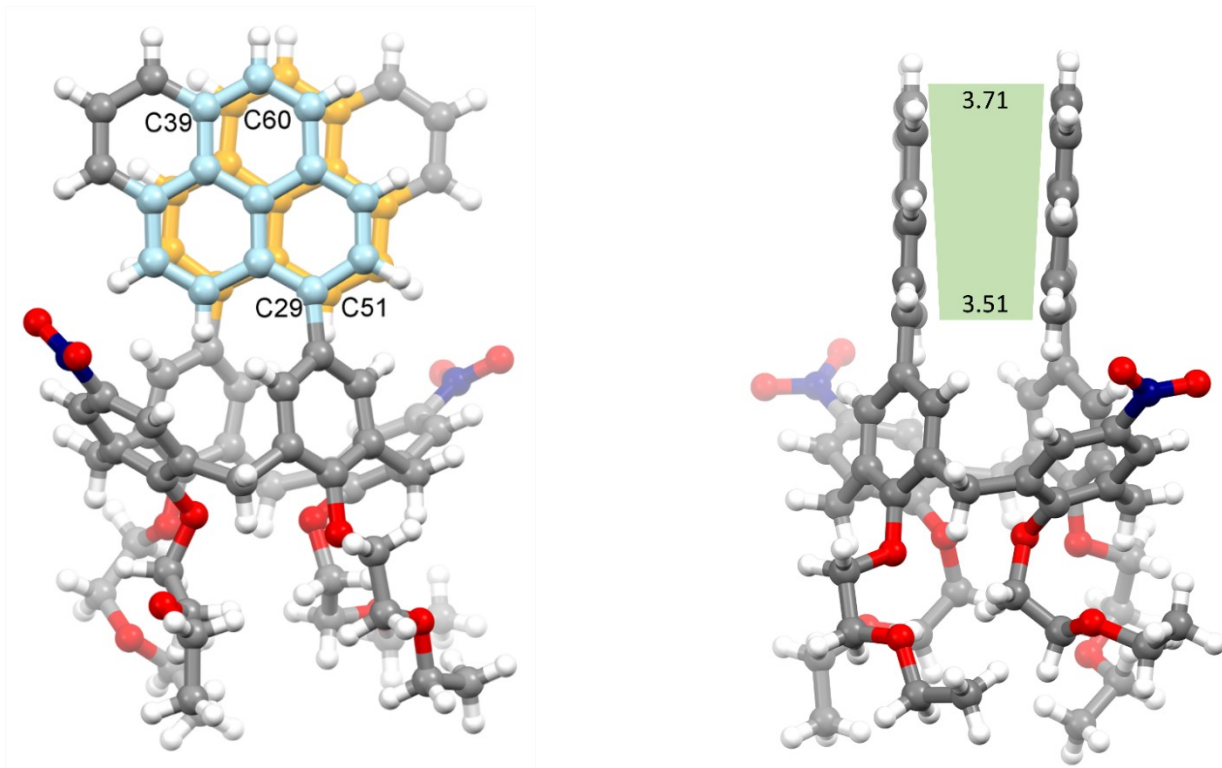


Fig. S2. Molecular structure of **7**, showing the partial π - π stacking between the two aromatic fragments. The partial overlap involving three out of four aromatic rings of each pyrene moiety is highlighted in yellow and cyan. The two pyrene units are slightly divergent. The closest contact is between the C(29) and C(51) atoms (3.51 Å), whereas the longest one is between the C(39) and C(60) atoms (3.71 Å).

2. Spectra

2.1. NMR Spectra

2.1.1. ^1H NMR spectrum of 7

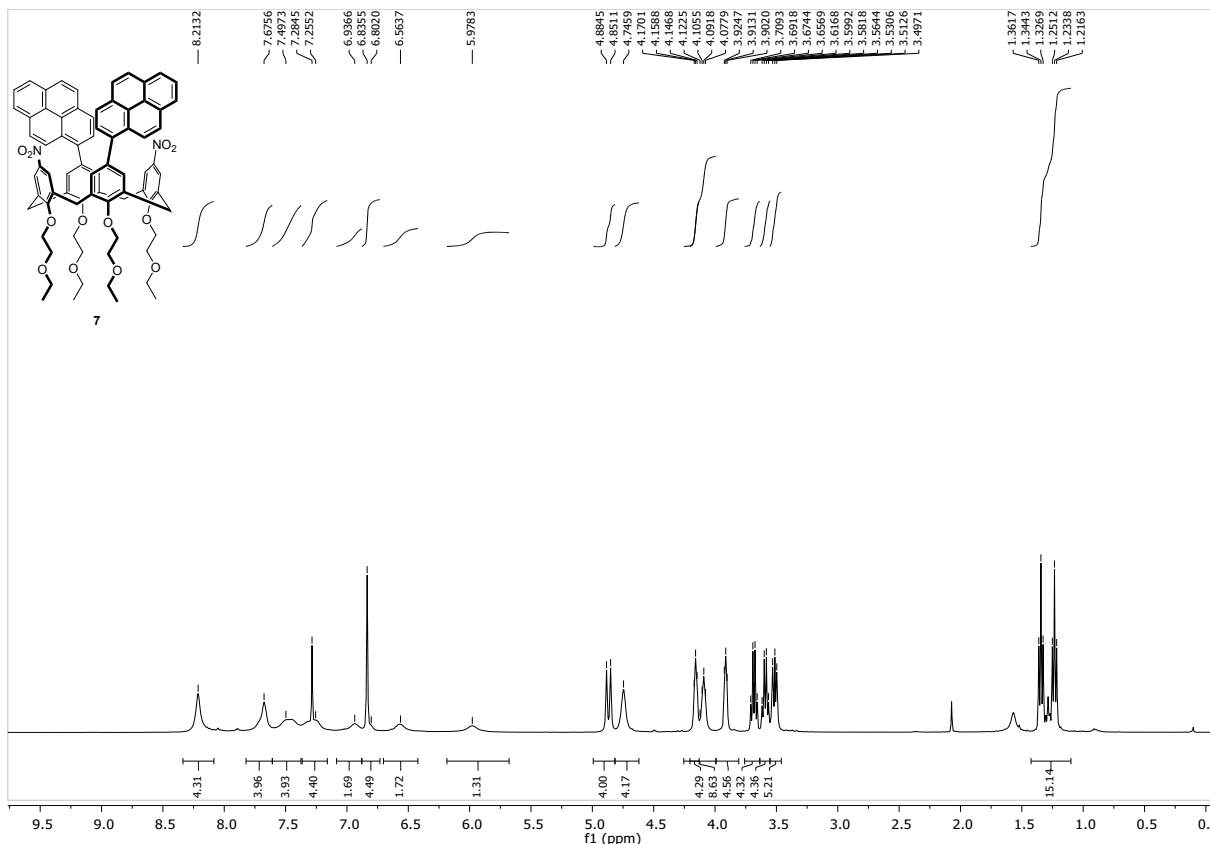


Fig. S3. ^1H NMR spectrum (400 MHz, CDCl_3) of calixarene 7. The peaks at 1.27, 2.07 and 4.12 ppm are due to residual ethyl acetate.

2.1.2. ^{13}C NMR spectrum of 7

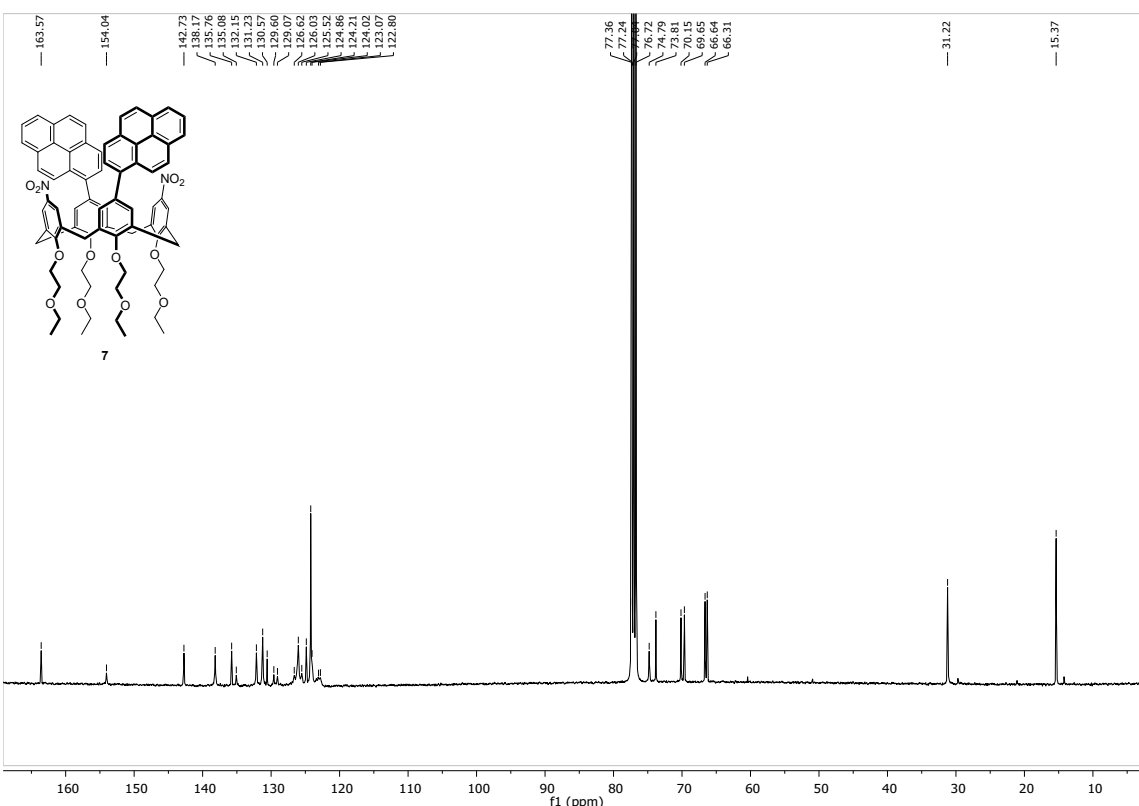


Fig. S4. ^{13}C NMR spectrum (100 MHz, CDCl_3) of calixarene 7. The small peaks at 14.2, 21.0, 60.5 and 171.1 ppm are due residual ethyl acetate. The signal at 29.7 ppm is due to grease and the peak at 50.4 ppm is due to residual methanol.

2.1.3. ^1H NMR spectrum of 3

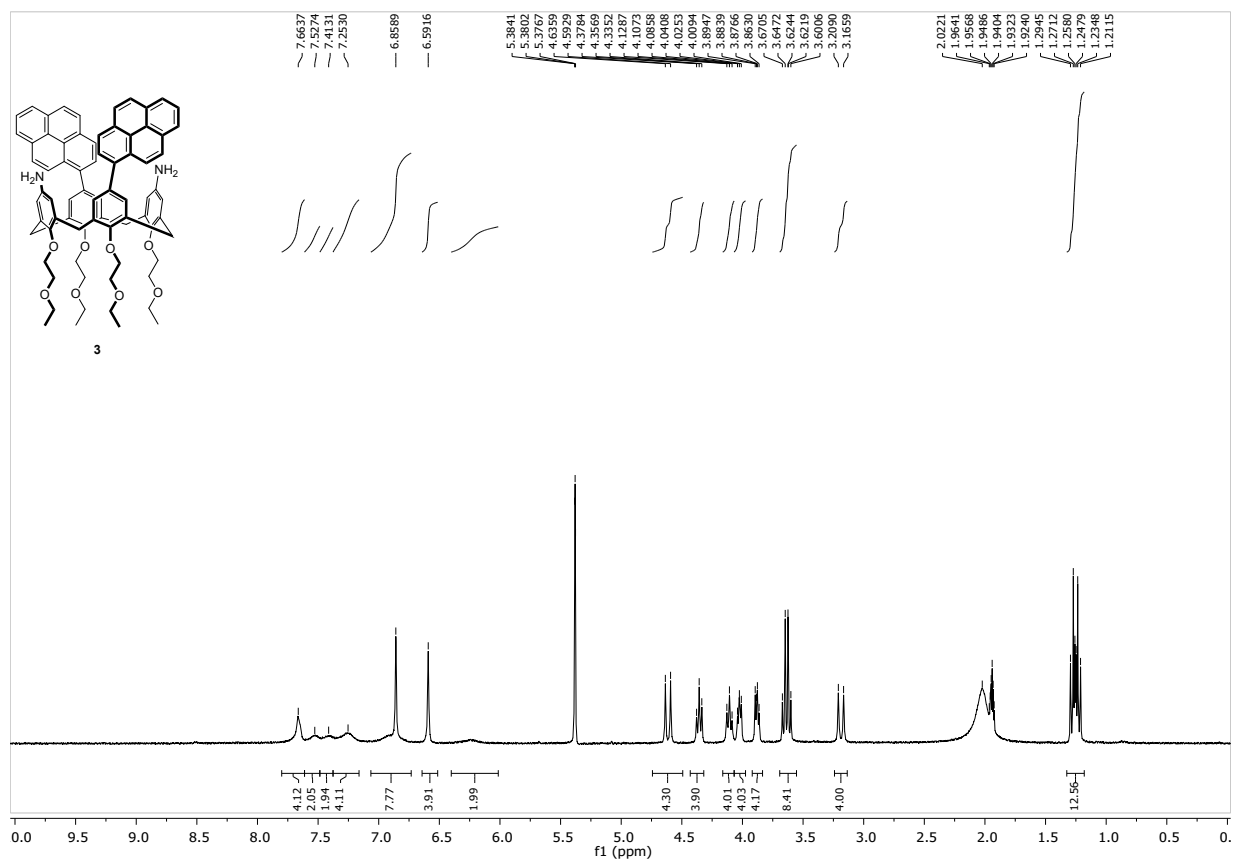


Fig. S5. ^1H NMR spectrum (400 MHz, $\text{CD}_2\text{Cl}_2/\text{CH}_3\text{CN}$) of calixarene 3.

2.1.4. ^{13}C NMR spectrum of 3

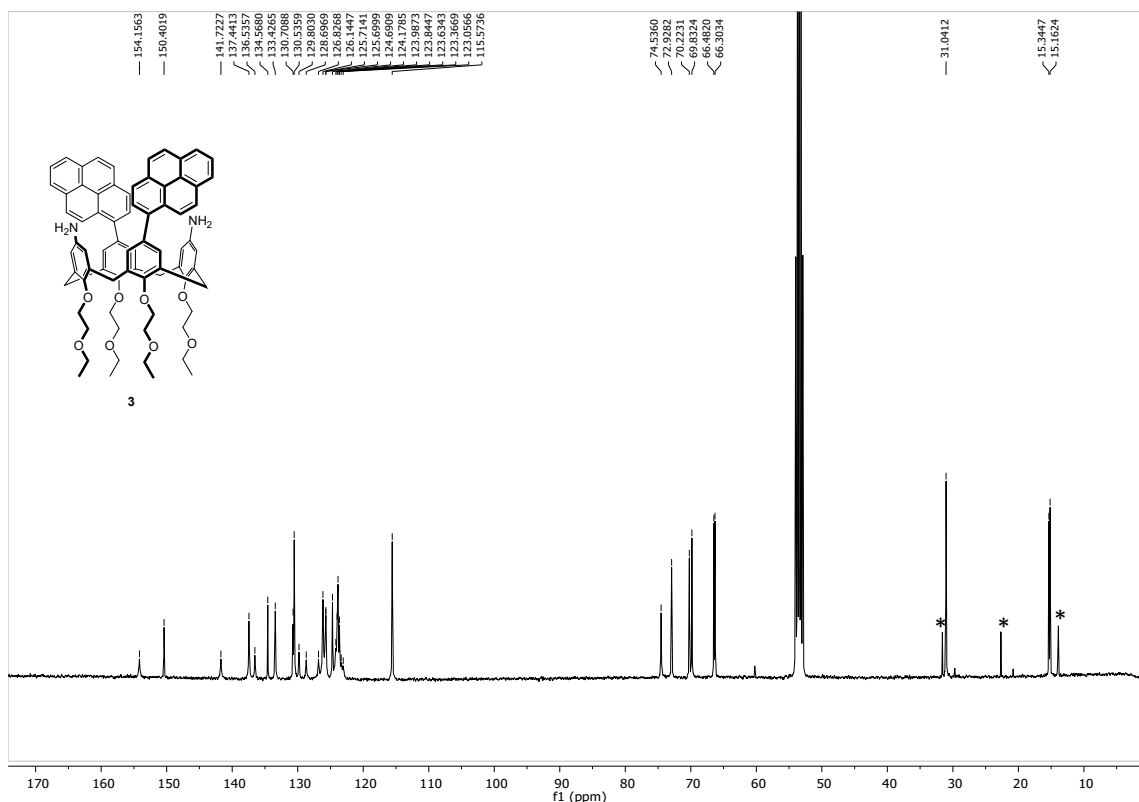


Fig. S6. ^{13}C NMR spectrum (100 MHz, CD_2Cl_2) of calixarene **3**. The peaks indicated by * are due to a solvent impurity (hexane). The small peaks at 14.4, 21.1, 60.6 and 171.2 ppm are due to residual ethyl acetate.

2.1.5. ^1H NMR Monitoring of the Reaction between 2.0 mM 3 and 4.0 mM 2

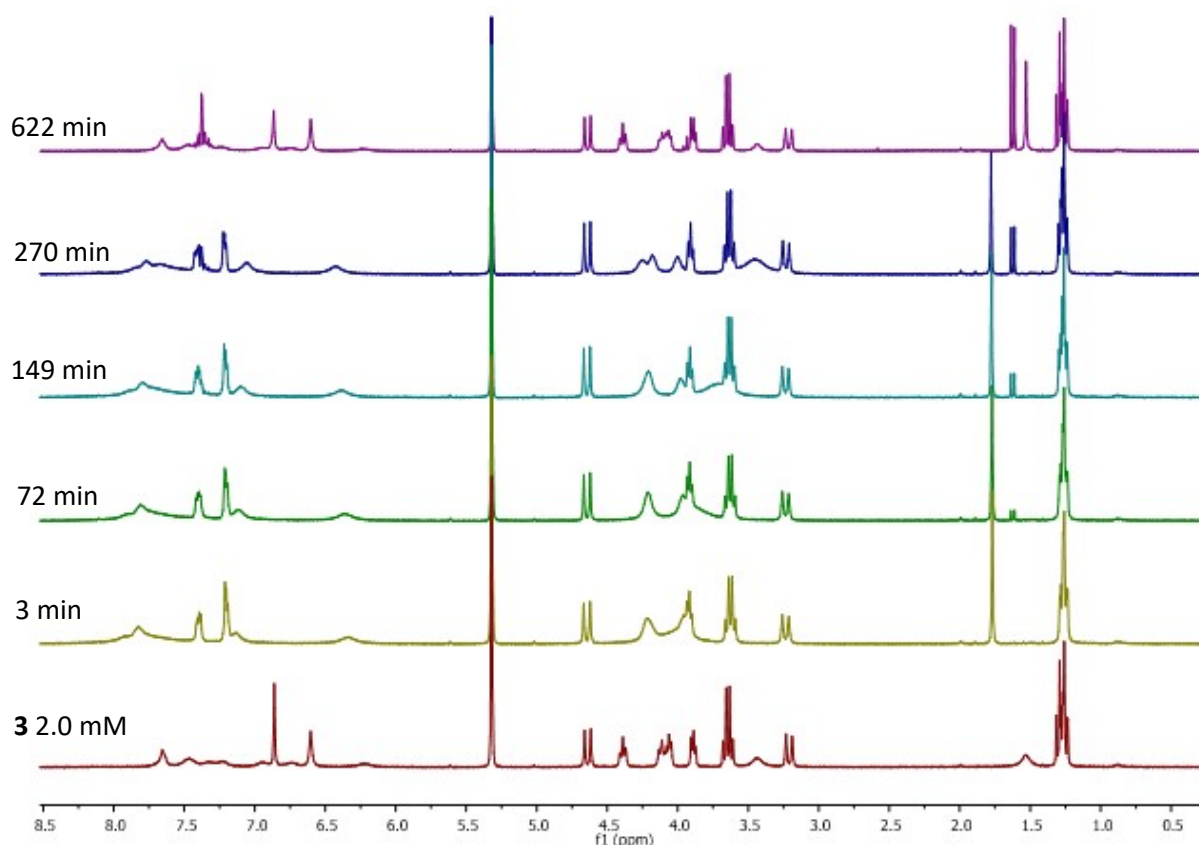


Fig. S7. ^1H NMR monitoring of the decarboxylation of 4.0 mM **2** catalysed by 2.0 mM **3**, (CD_2Cl_2 , 25 °C). The bottom trace is relative to 2.0 mM **3**, before the addition of **2**. Following spectra were recorded after the addition of acid **2**, at the given reaction time, upward increasing.

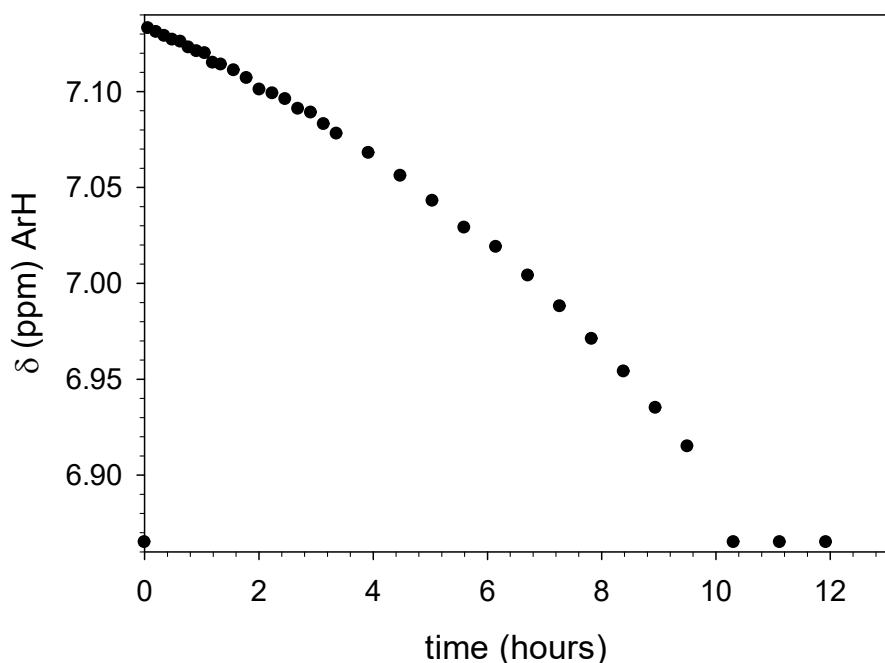
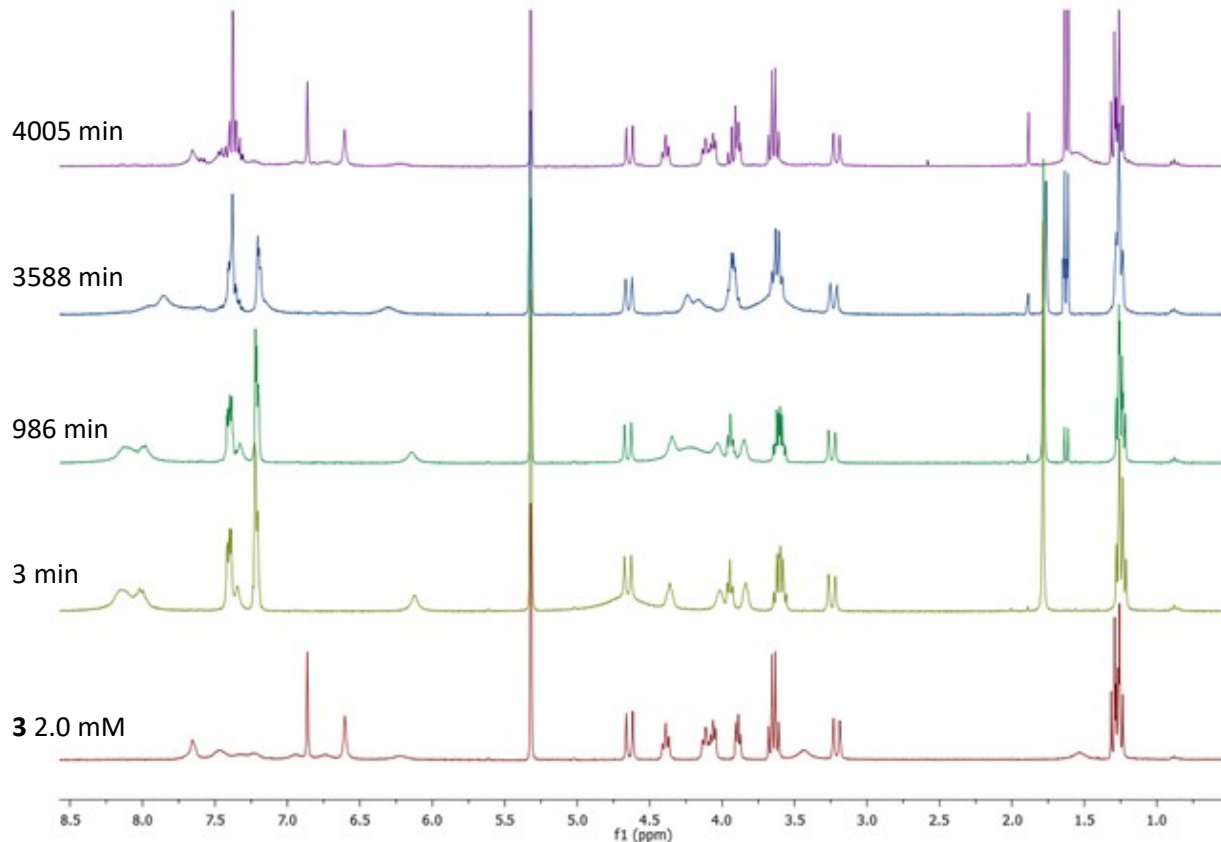


Fig. S8. ^1H NMR monitoring of the decarboxylation of 4.0 mM **2** catalysed by 2.0 mM **3**, (CD_2Cl_2 , 25 °C). The chemical shift of the pyrenyl substituted aromatic rings of **3** vs time is reported.



2.1.6. ¹H NMR Monitoring of the Reaction between 2.0 mM 3 and 10.0 mM 2

Fig. S9. ¹H NMR monitoring of the decarboxylation of 10.0 mM **2** catalysed by 2.0 mM **3**, (CD_2Cl_2 , 25 °C). The bottom trace is relative to 2.0 mM **3**, before the addition of **2**. Following spectra were recorded after the addition of acid **2**, at the given reaction time, upward increasing.

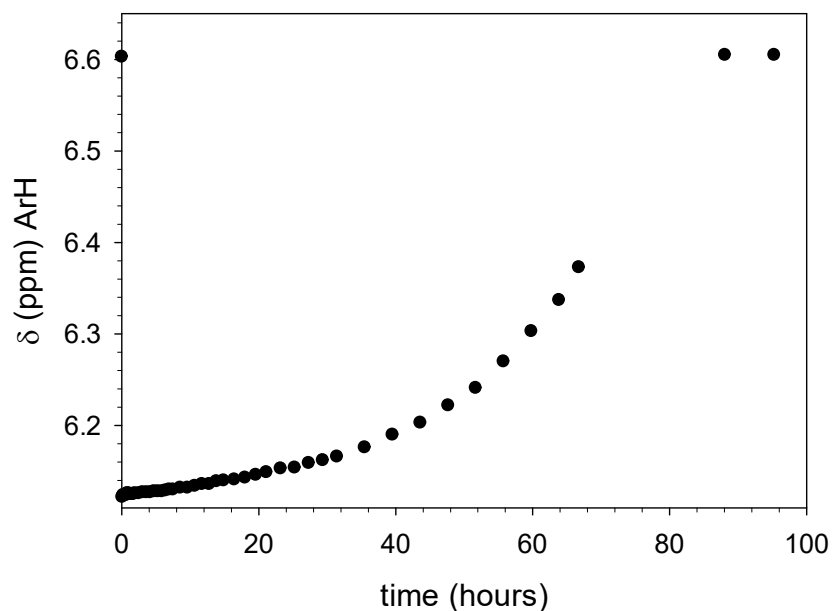
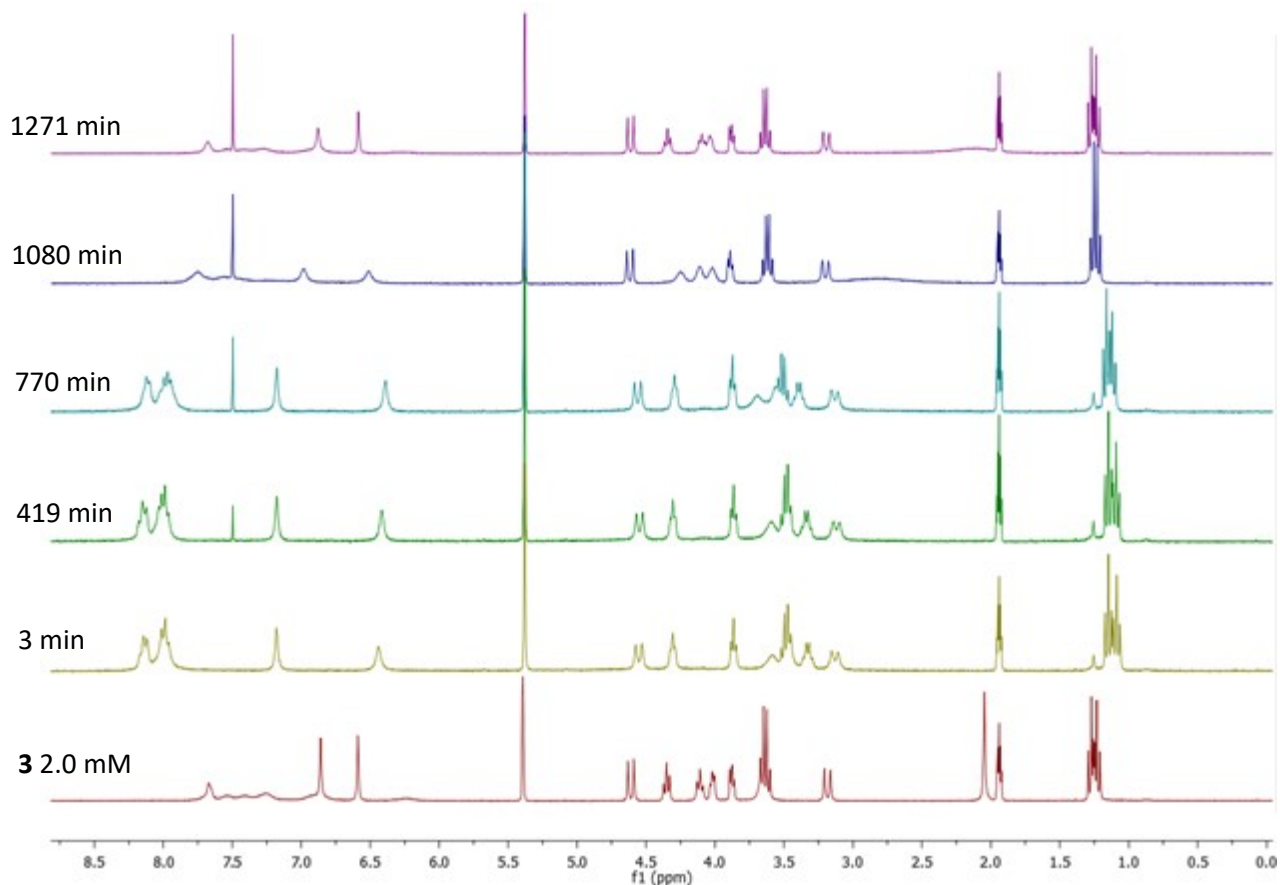


Fig. S10. ¹H NMR monitoring of the decarboxylation of 10.0 mM **2** catalysed by 2.0 mM **3**, (CD_2Cl_2 , 25 °C). The chemical shift of the amino substituted aromatic rings of **3** vs time is reported.



2.1.7. ¹H NMR Monitoring of the Reaction between 2.0 mM 3 and 4.6 mM 4

Fig. S11. ¹H NMR monitoring of the decarboxylation of 4.6 mM 4 catalysed by 2.0 mM 3, (CD₂Cl₂/CD₃CN 1/1, 25 °C). The bottom trace is relative to 2.0 mM 3, before fuel addition. Following spectra were recorded after the addition of acid 4, at the given reaction time, upward increasing.

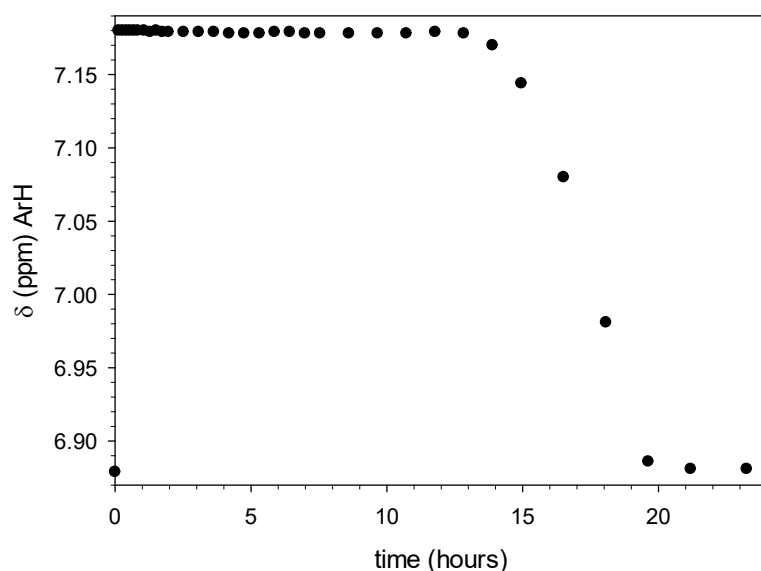
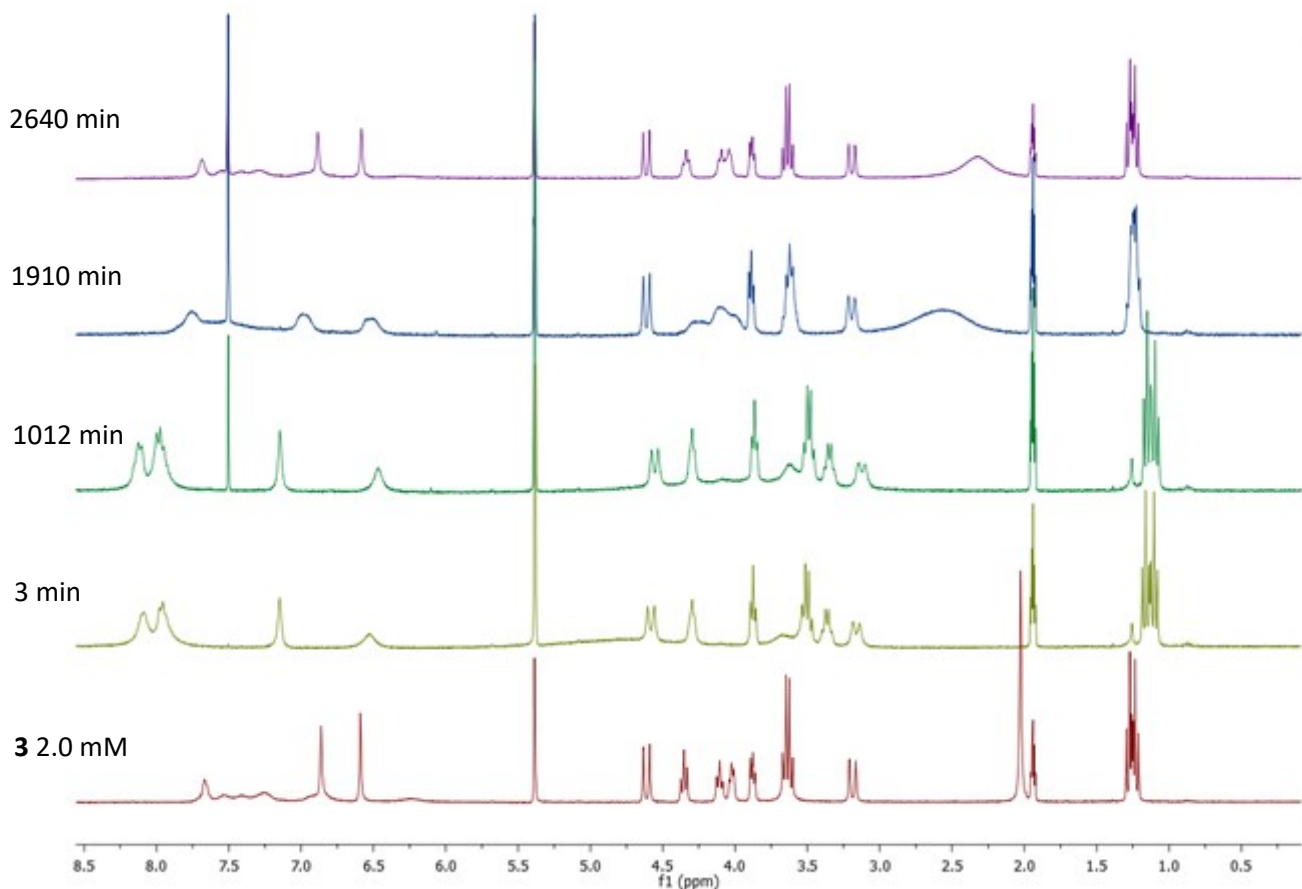


Fig. S12. ¹H NMR monitoring of the decarboxylation of 4.6 mM 4 catalysed by 2.0 mM 3, (CD₂Cl₂/CD₃CN 1/1, 25 °C). The chemical shift of the pyrenyl substituted aromatic rings of 3 vs time is reported.



2.1.8. ¹H NMR Monitoring of the Reaction between 2.0 mM 3 and 8.0 mM 4

Fig. S13. ¹H NMR monitoring of the decarboxylation of 8.0 mM 4 catalysed by 2.0 mM 3, (CD₂Cl₂/CD₃CN 1/1, 25 °C). The bottom trace is relative to 2.0 mM 3, before the addition of 2. Following spectra were recorded after the addition of acid 4, at the given reaction time, upward increasing.

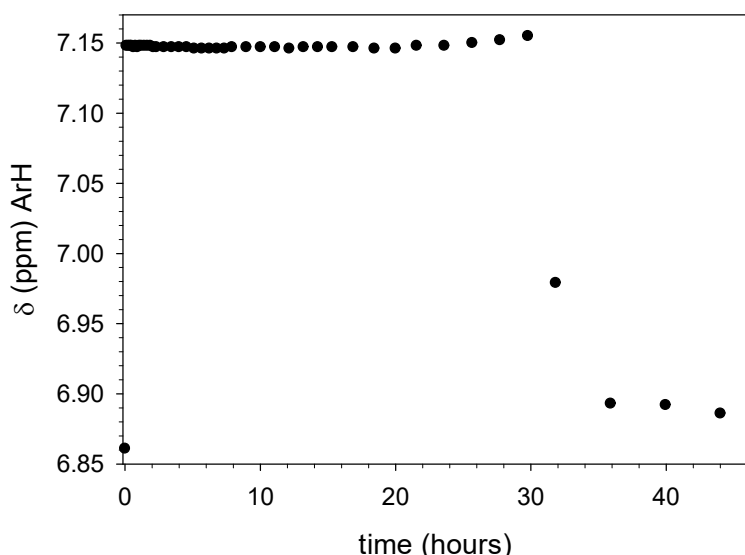


Fig. S14. ¹H NMR monitoring of the decarboxylation of 8.0 mM 4 catalysed by 2.0 mM 3, (CD₂Cl₂/CD₃CN 1/1, 25 °C). The chemical shift of the pyrenyl substituted aromatic rings of 3 vs time is reported.

2.1.9. Comparison between ^1H NMR of 3H^+ after addition of CF_3COH and $\text{CCl}_3\text{CO}_2\text{H}$

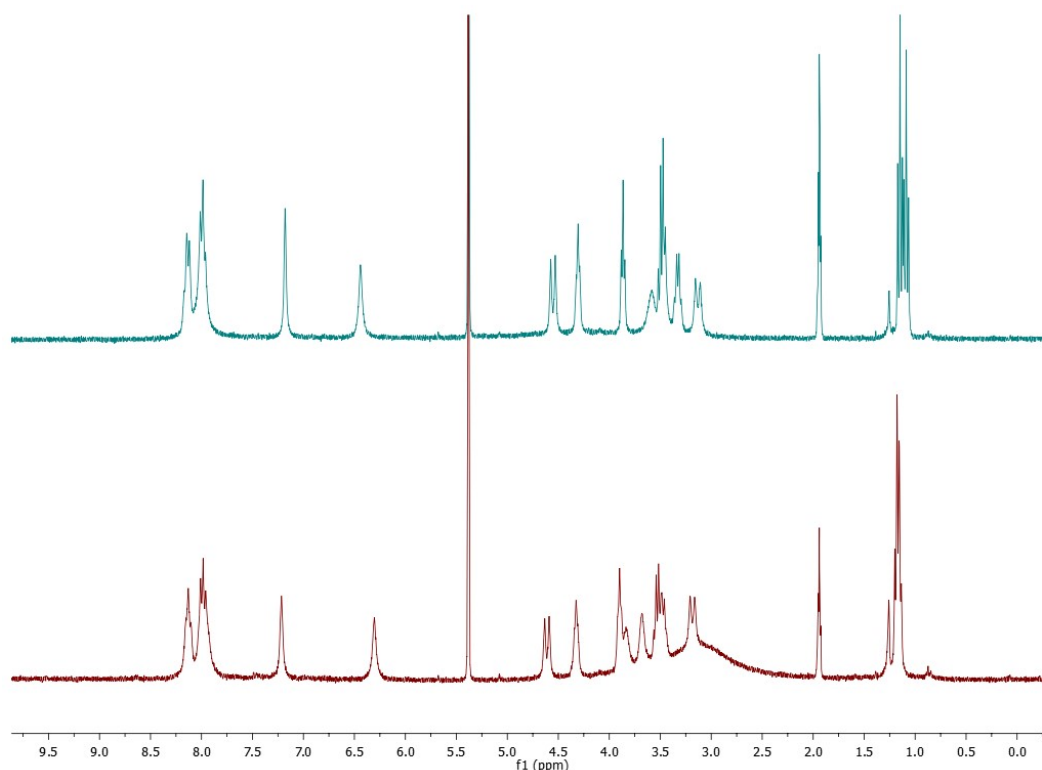


Fig. S15. ^1H NMR ($\text{CD}_2\text{Cl}_2/\text{CD}_3\text{CN}$ 1/1, 25 °C) Comparison of the spectra obtained after the addition 2 mol equivs of TFA to 2.0 mM **3** (bottom trace) and, immediately after the addition of 2.3 mol equivs of **4** to 2.0 mM **3** (top trace).

2.2 Emission spectra

2.2.1. Fluorescence emission spectrum of 0.15 mM 3

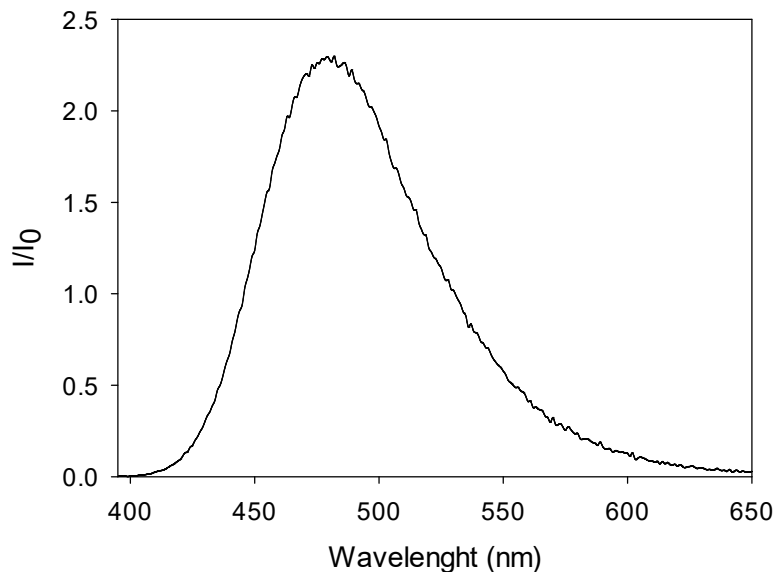


Fig. S16. Fluorescence spectrum of 0.15 mM **3**, ($\text{CH}_2\text{Cl}_2/\text{CH}_3\text{CN}$ 1/1, 25 °C, $\lambda_{\text{exc}} = 385$ nm, slit = 1 nm).

2.2.2. Fluorescence emission spectrum of 0.15 mM 7

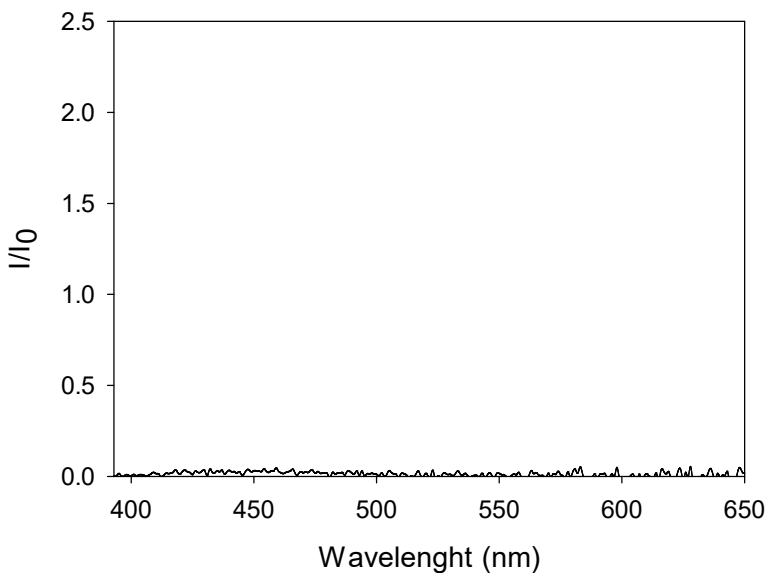


Fig. S17. Fluorescence spectrum of 0.15 mM **7**, ($\text{CH}_2\text{Cl}_2/\text{CH}_3\text{CN}$ 1/1, 25 °C, $\lambda_{\text{exc}} = 383$ nm, slit = 1 nm).

2.2.3. Fluorescence emission spectrum of 5.0 μM 3

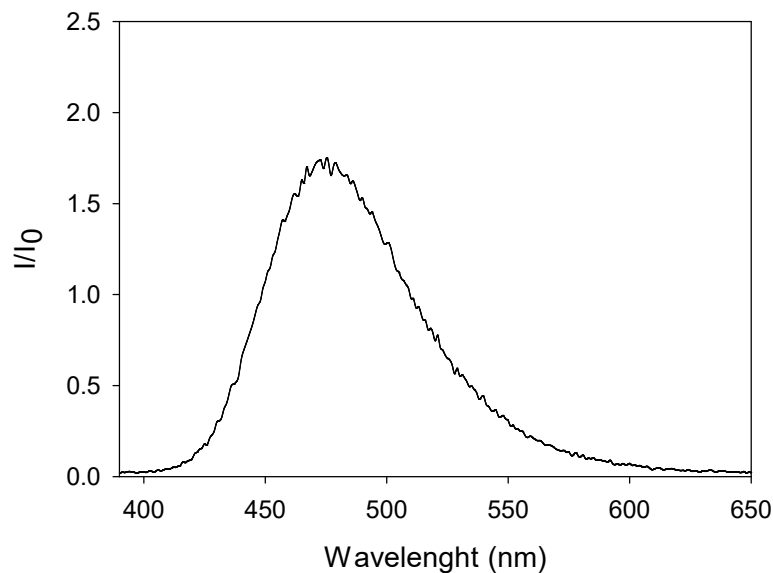


Fig. S18. Fluorescence spectrum of 5.0 μM 3, ($\text{CH}_2\text{Cl}_2/\text{CH}_3\text{CN}$ 1/1, 25 °C, $\lambda_{\text{exc}} = 353$ nm, slit = 1 nm).

2.2.4. Fluorescence emission spectrum of 5.0 μM 7

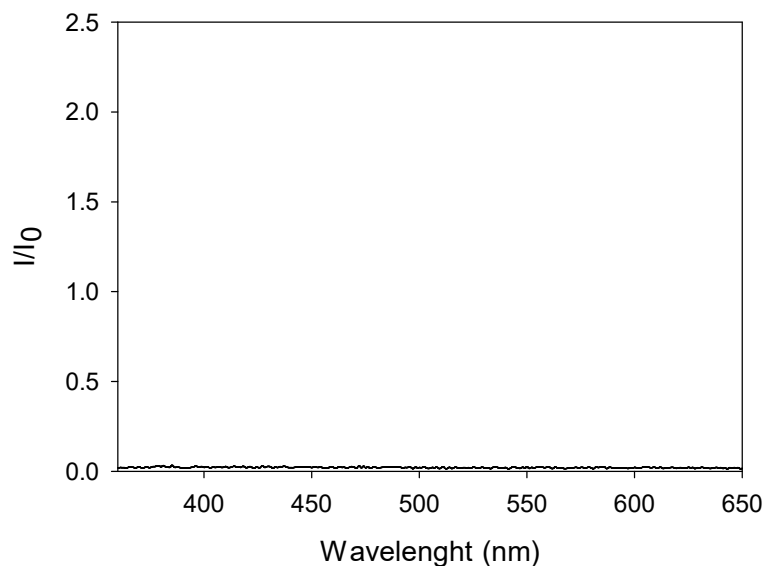


Fig. S19. Fluorescence spectrum of 5.0 μM 7, ($\text{CH}_2\text{Cl}_2/\text{CH}_3\text{CN}$ 1/1, 25 °C, $\lambda_{\text{exc}} = 345$ nm, slit = 1 nm).

2.2.5. Fluorescence emission spectrum of 5.0 μ M 7

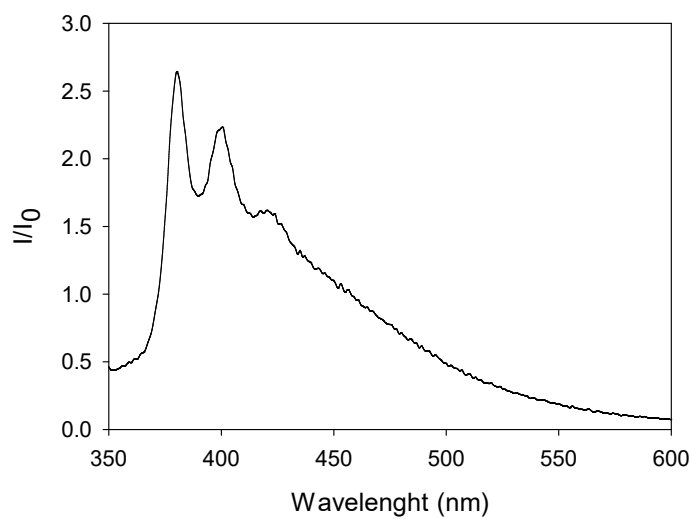


Fig. S20. Fluorescence spectrum of 5.0 μ M 7, (CH_2Cl_2 , 25 °C, $\lambda_{\text{exc}} = 345$ nm, slit = 5 nm).

2.2.6. Fluorescence emission spectrum of 2.50 μ M 3 + 2.50 μ M $\text{CF}_3\text{CO}_2\text{H}$

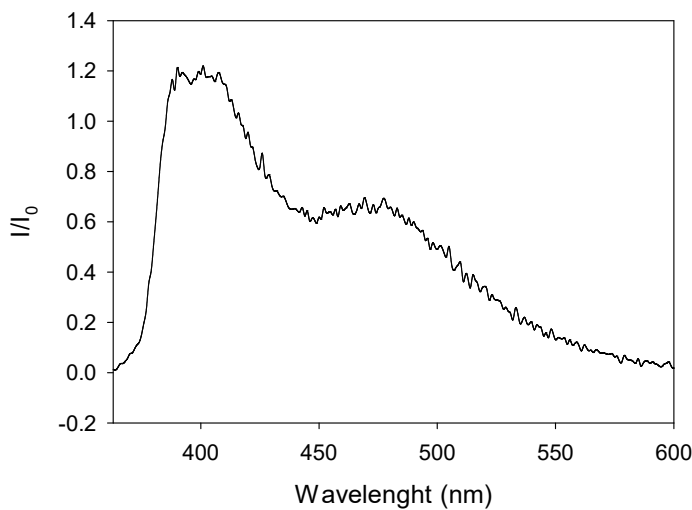


Fig. S21. Fluorescence spectrum of 2.50 μ M 3 + 2.50 μ M TFA in $\text{CH}_2\text{Cl}_2/\text{CH}_3\text{CN}$ 1/1.

2.3 UV-Vis absorption spectra

2.3 UV-Vis absorption spectra of 2.50 μM in the presence and absence of 2.50 μM $\text{CF}_3\text{CO}_2\text{H}$

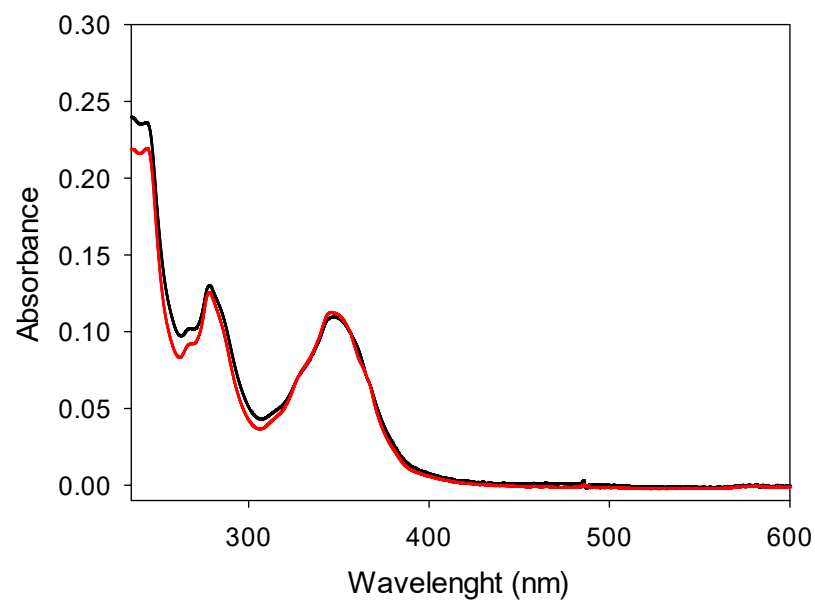


Fig. S22. UV-Vis absorption spectra of 2.50 μM **3** (black) and 2.50 μM **3** + 2.50 μM TFA (red) in $\text{CH}_2\text{Cl}_2/\text{CH}_3\text{CN}$ 1/1.

2.4 Excitation spectra

2.4.1 Excitation spectra of 2.50 μM 3 + 2.50 μM CF₃CO₂H

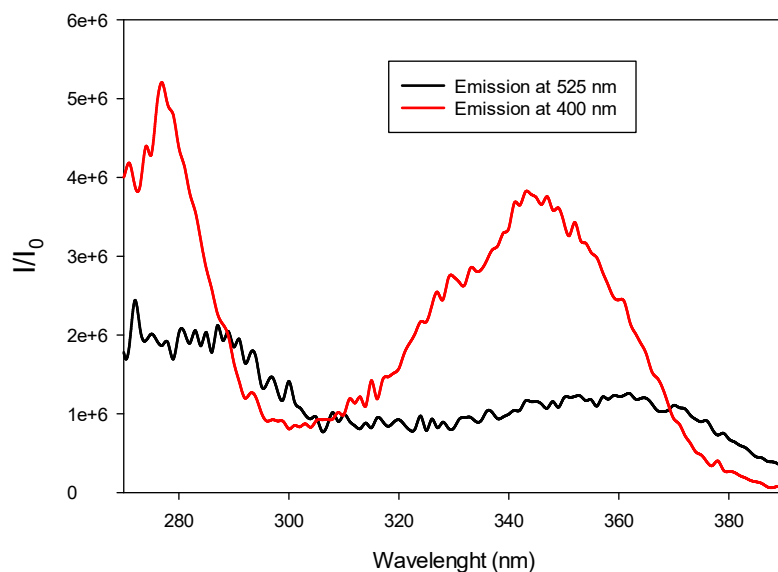


Fig. S23. Excitation spectra of 2.50 μM 3 + 2.50 μM TFA in $\text{CH}_2\text{Cl}_2/\text{CH}_3\text{CN}$ 1/1 monitored at 400 nm (red trace) and at 525 nm (black trace).

Excitation spectra monitoring at the monomer and at the excimer emission can be used to investigate the origin of the pyrene dimer. If the spectra are identical, then the pyrene dimer is an excimer (a dimer formed in the excited state). If, on the contrary, one of the spectra is shifted, the dimer is already formed in the ground-state. Some authors⁶ consider the first dimer a “dynamic excimer” and the second a “static” one.

The spectra in Fig. S23 show that the excitation spectrum monitored at 525 nm is red-shifted with respect to that monitored at 400 nm, suggesting that the excimer band is emitted by a pyrene dimer formed at the ground-state (“static excimer”).

3. References

1. P. Timmerman, W. Verboom, D. N. Reinhoudt, A. Arduini, S. Grandi, A. R. Sicuri, A. Pochini and R. Ungaro, *Synthesis*, 1994, **2**, 185.
2. Bruker (2012). SMART. Bruker AXS Inc., Madison, Wisconsin, USA.
3. L. Krause, R. Herbst-Irmer, G. M. Sheldrick and D. Stalke, *J. Appl. Cryst.* 2015, **48**, 3.
4. G. M. Sheldrick, *Acta Cryst. A*, 2015, **71**, 3.
5. C. F. Macrae, I. Sovago, S. J. Cottrell, P. T. A. Galek, P. McCabe, E. Pidcock, M. Platings, G. P. Shields, J. S. Stevens, M. Towler and P. A. Wood, *J. Appl. Cryst.*, 2020, **53**, 226.
6. (a) F. M. Winnik, , *Chem. Rev.* 1993, **93**, 587. (b) S .K. Kim, J. H. Bok, R. A. Bartsch, J. Y. Lee, J. S. Kim, *Org. Lett.* 2005, **22**, 4839.